



Influence of chemical bonding on thermal contact resistance at silica interface: A molecular dynamics simulation



Zun Huang^a, Congliang Huang^{a,b,*}, Dongxu Wu^a, Zhonghao Rao^{a,*}

^a School of Electrical and Power Engineering, China University of Mining and Technology, Xuzhou 221116, China

^b Department of Mechanical Engineering, University of Colorado, Boulder, CO 80309-0427, USA

ARTICLE INFO

Keywords:

Thermal contact resistance
Molecular dynamics simulation
Chemical bonding
Silica

ABSTRACT

The chemical bonding is usually not avoidable at a welding or fusion interface and sometimes is desirable to enhance the mechanical strength, while it might strongly affect the thermal contact resistance which plays a critical role in hindering heat dissipation of electronic devices. In this paper, we employ a non-equilibrium molecular dynamics method to study the effect of chemical bonding on the thermal contact resistance. Results show that the chemical bonding can greatly affect the thermal contact resistance. With the increase of the chemical bonding ratios, the thermal contact resistance firstly drops dramatically until arrives at a bonding ratio of about 20% where the thermal contact resistance is only about 15% that with a bonding ratio of 0%, and then gradually decreases to 0. Analyzing the spectral energy density of phonons at the interface, we conclude that the increase of the phonon velocity should be responsible for the decrease of the thermal contact resistance. By simulating the thermal contact resistance of silica with different morphologies (crystalline or amorphous silica), we found that different morphologies could lead to different thermal contact resistances, although this difference is less than 6%. This study is expected to provide references for managing thermal transport at a welding or fusion interface.

1. Introduction

The chemical bonding is usually not avoidable at a welding or fusion interface and sometimes is desirable to enhance the mechanical strength. To reinforce the structure strength, the chemical bonding has been widely established with a high pressure and/or a high temperature to bond metals, alloys, ceramics and composites [1–3], and the chemical bonding can also occur in a process of annealing [4]. Besides above methods, severe mechanical stress was also applied to build an interfacial bridging by Si–O–Si bonds between spherical Si nanocrystals and a α -SiO₂ matrix [5]. Although there are always chemical bonds at interfaces, the effect of chemical bonding on thermal contact resistance has been rarely investigated yet. More importantly, the chemical bonding can greatly affect the thermal contact resistance, while thermal contact resistance plays a critical role in hindering heat dissipation in electronic devices.

Numerous studies have already been performed to probe methods to reduce the thermal contact resistance [6–9]. Most recently, it is reported that the presence of chemical bonds could greatly decrease the thermal contact resistance between amorphous silica nanoparticles [10]. In this paper, the chemical bonding effect on thermal contact

resistance is further studied. Considering the wide application of silica in thermal insulation [11–13] (silica aerogel or silica composites) and electronic packaging [14] (silica packing material), the thermal contact resistance between crystalline-crystalline, amorphous-crystalline, and amorphous-amorphous silica is focused in this paper. The α -SiO₂ is applied as the crystalline silica in this work.

The non-equilibrium molecular dynamics (NEMD) simulation is firstly applied in this work to get the temperature distribution along heat transfer direction with a given heat flux, where a temperature jump will happen at the interface because of the contact resistance [6,15]. Then, according to the definition, the thermal contact resistance is calculated by the temperature drop divided by the heat flux. Finally, analyzing the cumulative correlation factor (CCF) which depicts mismatch of vibrational density of states (DOSs) between two materials, and radial distribution function (RDF) which represents the difference of structures, the structure dependence of thermal contact resistance is explained. The spectral energy density (SED) of phonons at the interface is also calculated to illustrate the effect of chemical bonding on phonons. Results turn out that the chemical bonding can greatly affect the thermal contact resistance. This study is expected to provide references for managing thermal transport at a welding or fusion

* Corresponding authors at: School of Electrical and Power Engineering, China University of Mining and Technology, Xuzhou 221116, China.
E-mail addresses: huangcl@cumt.edu.cn (C. Huang), raozhonghao@cumt.edu.cn (Z. Rao).

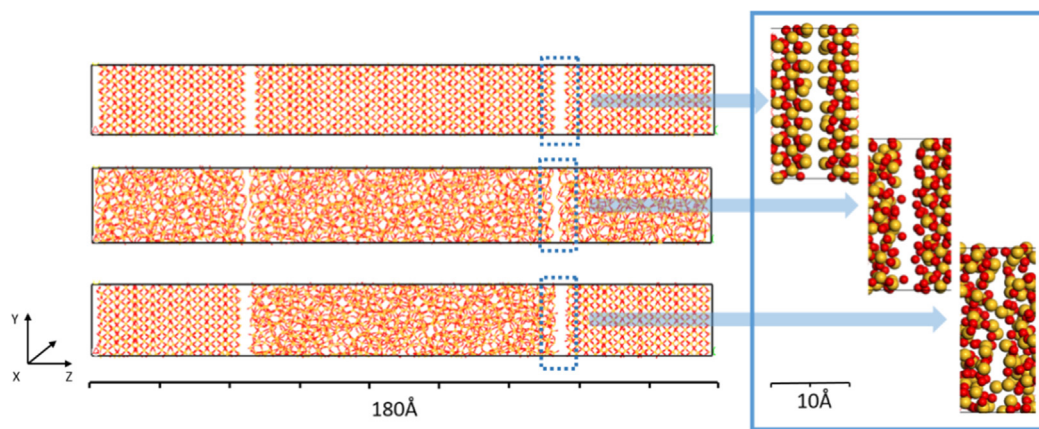


Fig. 1. Structures used in our simulation (interface without chemical bonds is shown here). The upper, middle and lower panels show crystalline-crystalline, amorphous-amorphous, and crystalline-amorphous interface configurations respectively.

interface. With a known thermal contact resistance, the revealed relationship between the thermal contact resistance and bonds can be also applied to estimate the interface structural strength.

2. Simulation and calculation methods

Sandwich structures are built to investigate the thermal contact resistance with Material Studio package, as shown in Fig. 1. Every structure contains about 5000 atoms. As that done in the previous work [16], an interface distance of about 2 Å is applied here. The structure size used in our simulation is summarized in Table 1. For comparison, three kinds of silica contact interface are studied, the amorphous-amorphous, crystalline-crystalline and crystalline-amorphous interfaces.

For convenience, the interfacial bonding ratio is defined as the percentage of atoms connected through Si–O–Si bonds to other-side atoms at interface. The calculation method of the interfacial bonding ratio is added in Appendix A. To illustrate the influence of chemical bonds on thermal contact resistance, different bonding ratios are applied, i.e., 0, 6.25, 12.5, 25, 50 and 75%. Chemical bonds are distributed randomly at interface in our simulation, as that done in Ref. [17]. A crystalline-crystalline configuration with a bonding ratio of 6.25% is shown in Fig. 2.

In the present work, the COMPASS potential [18–20] which is the first ab initio force field and has been validated to be capable of accurately predicting structural and thermophysical properties within a broad range of organic and inorganic substances, is used to describe the interactions between atoms. The potential function is exhibited in Appendix B. In general, the terms in the potential function could be divided into bonded interaction terms and non-bonded interaction terms. While there are no bonds at interface, two materials at interface are connected by van der Waals force and Coulomb force described by extended L-J equation,

$$V(r) = \sum_{ij} \varepsilon_{ij} \left[2 \left(\frac{\sigma_{ij}}{r_{ij}} \right)^9 - 3 \left(\frac{\sigma_{ij}}{r_{ij}} \right)^6 \right] + \frac{1}{4\pi\epsilon_0} \sum_{ij} \frac{q_i q_j}{r_{ij}} \quad (1)$$

where r is the distance between two atoms located at different side of interface, q_i and q_j are the signed magnitudes of the charges, ϵ_0 is

Table 1
Structure size applied in the simulation.

Structure	X direction (Å)	Y direction (Å)	Z direction (Å)
Crystalline-crystalline	17.50	20.21	179.24
Amorphous-amorphous	20.95	20.95	171.41
Crystalline-amorphous	19.10	20.42	175.31

Coulomb's constant, $\sigma_{ij} = \left[\frac{\sigma_i^6 + \sigma_j^6}{2} \right]$ and $\varepsilon_{ij} = 2\sqrt{\varepsilon_i \varepsilon_j} \frac{\sigma_i^3 \sigma_j^3}{\sigma_i^6 + \sigma_j^6}$, where ε is energy parameter, σ is the distance parameter. The L-J parameters are taken from Ref. [18] listed in Table 2.

Before NEMD simulation, the configurations should be optimized to confirm the energy minimization. Geometry optimization is firstly performed on the initial configuration, and a NPT ensemble is applied to release the structure interstress for 50 ps with a time step of 0.5 fs, at a pressure of 0.1 MPa controlled by Berendsen method and a temperature of 300 K controlled by Nose-Hoover thermostat. Then, the systems are equilibrated for 500 ps with a time step of 0.2 fs at 300 K under the NVT ensemble. We double-check that the total energy has reached minimum and convergence has been reached at the end of NVT ensemble to make sure that our systems have already been equilibrated.

Finally, with a periodic boundary applied in the X, Y and Z directions, where Z direction is set to be the heat transfer direction, the NEMD method [21–25] is applied to get the temperature profile. In this work, with every 10 time steps, the velocity of the fastest atom in “cold” slab is replaced by the velocity of the slowest atom in “hot” slab, and vice versa. Consequently the “cold” slab becomes colder, whereas the temperature of the “hot” slab increases. The system will react by flowing energy from the hot to the cold region. Eventually a steady state sets in when the energy exchanged offsets the energy flowing back with a temperature gradient over the space between the two slabs. In our paper, the simulation box is firstly divided into N slabs ($N = 40$ in this paper) in the heat transfer direction, the first slab (slab 0) is defined as the “hot” slab, and the slab $N/2$ is defined as the “cold” slab. The temperature T in each slab is calculated by,

$$T = \frac{1}{3nk_B} \sum_{i=1}^n m_i v_i^2 \quad (2)$$

where the summation extends over the atoms i with masses m_i and velocities v_i . k_B is Boltzmann's constant. The heat flux is created by exchanging velocities of particles in “cold” and “hot” slabs. As what is introduced above, the “cold” slab donates its “hottest” particles with the highest kinetic energy to the “hot” slab in exchange for the latter's “coolest” particles with the lowest kinetic energy. This process leads to a temperature difference between the cool and the hot slab, and the temperature profile is given by the temperatures in the intervening slabs from 1 to $N/2-1$ and from $N/2+1$ to $N-1$, where the temperature is obtained by averaging temperatures within last 1000 simulation steps. With a time step of 0.2 fs, a total simulation time of 0.5 ns is taken to get a steady temperature distribution. To test whether the simulation system reaches the steady state or not, the effective thermal conductivity of the whole structure is also calculated and shown in Fig. 4. It shows that 0.5 ns are long enough to get a steady-state. After getting the temperature drop ΔT at the interface, the

Download English Version:

<https://daneshyari.com/en/article/7957603>

Download Persian Version:

<https://daneshyari.com/article/7957603>

[Daneshyari.com](https://daneshyari.com)